Meteorol. Atmos. Phys. 69, 179–193 (1999)

Meteorology and Atmospheric Physics

Centro de Previsão de Tempo e Estudor Climáticos
Instituto Nacional de Pesquisas Espaciais, Brazil

High-frequency Patterns of the Atmospheric Circulation over the Southern Hemisphere and South America

I. F. A. Cavalcanti and **M. T. Kayano**

With 13 Figures

Received August 10, 1998

Summary

Daily 500-hPa geopotential height and 250-hPa meridional wind reanalyzed data obtained from the National Centers for Environmental Prediction are used to document austral winter (May to September) and summer (November to March) high-frequency variability in the Southern Hemisphere (SH) midlatitudes for the 1990–1994 period. Empirical orthogonal function (EOF) technique is used to determine the high-frequency patterns for these variables in selected areas. The high-frequency anomalous 500-hPa geopotential height patterns for two areas in the SH midlatitudes (the zonally global domain and the western hemisphere) and the high-frequency anomalous 250-hPa meridional wind patterns in the western hemisphere between 15° N and 70° S are discussed. The high-frequency winter and summer patterns for both variables feature a wavetrain structure in the SH midlatitudes which is related to synoptic-scale systems, such as cyclones and anticyclones associated with frontal zones. The dominant high-frequency patterns in the SH midlatitudes manifest in the eastern hemisphere while the secondary ones appear in the southeastern Pacific. Analysis of the western hemisphere data reveal that the wavetrain in the South American sector extends northeastward over the continent, thus affecting the regional weather conditions. An important result presented here concerns the preference of the intense synoptic systems in the eastern hemisphere and in the southeastern Pacific to occur in a sequential instead of an intermittent fashion. This result might have a potential for being used in weather monitoring.

1. Introduction

The first works on the behavior and characteristics of transient eddies in the Southern Hemisphere (SH) date from the beginning of the 80's. Trenberth (1981, 1982), using hemispheric data from the World Meteorological Centre in Melbourne, Australia, studied the role played by the SH transient eddies on the momentum fluxes. Afterwards, Trenberth (1991) using data from the European Centre for Medium Range Weather Forecasts (ECMWF) provided more information on the SH storm tracks which are zonally oriented along 50° S throughout the year. More recently, Berbery and Vera (1996) using six years of the ECMWF daily analyses studied the structure and evolution of the SH synoptic-scale fluctuations during winter. They found wave packets with the upstream centers decaying and new centers growing downstream. Also, they suggested that the downstream development contributes to the evolution of the synoptic-scale waves in the SH storm tracks.

Several studies have shown that the synoptic systems frequently cause weather changes over South America thus resulting in a seasonal variability of precipitation for this region. Most of these systems, detected in satellite images, occur either throughout the year, as frontal systems moving across the continent (Kousky, 1979; Kousky and Cavalcanti, 1997) and midlatitude upper level cyclonic vortices over the southeastern Pacific or during specific seasons, like tropical features manifesting themselves over the continent mainly during the austral

summer as the South Atlantic Convergence Zone (SACZ) (Kodama, 1992), Bolivian high (Virji, 1981) and upper level cyclonic vortices over northeast Brazil (Kousky and Gan, 1981; Kayano et al., 1997). From all these, frontal zones are the major systems responsible for the high-frequency variability over South America (Kousky and Cavalcanti, 1997). Regional weather conditions may also be affected by the passage of troughs, cyclogeneses and frontogeneses in the southern part of the continent (Gan and Rao, 1991, 1994) and by the occurrence of blocking situations over the South American sector and neighboring areas (Kayano and Kousky, 1990; Sinclair,1996).

The reanalyzed homogeneous (in terms of the model physics and resolution) data are appropriated for diagnostic studies of the atmospheric variability on several time-scales in different regions of the globe. The present study used the 500-hPa geopotential height and 250-hPa meridional wind reanalyzed fields obtained from the National Centers for Environmental Prediction to investigate the high-frequency variability in the SH midlatitudes and in the South American region, in particular. A better understanding of the high-frequency variability is important to improve weather monitoring and forecasting, especially for areas where many activities are strongly weather dependent, as is the case for southern South America.

2. Data and Methodology

The data used in this study consist of 17 years (1979–1995) of reanalyzed daily averaged 500-hPa geopotential height and 250-hPa meridional wind fields produced by the Climate Data Assimilation System (CDAS) Reanalysis Project (Kalnay et al., 1996). These data have a resolution of 2.5° in both latitude and longitude. Daily anomalies are calculated by removing the daily climatology, based on the first four harmonics, for the same 17-year period. The anomaly time series are filtered using a Lanczos high-pass filter (Duchon, 1979) with 25 weights and cutoff frequency of 10 day^{-1}. The frequency response of this filter (Fig. 1) shows that only high-frequency fluctuations are retained in the filtered time series.

The high-frequency anomalous 500-hPa geopotential height patterns are determined performing empirical orthogonal function (EOF) analyses

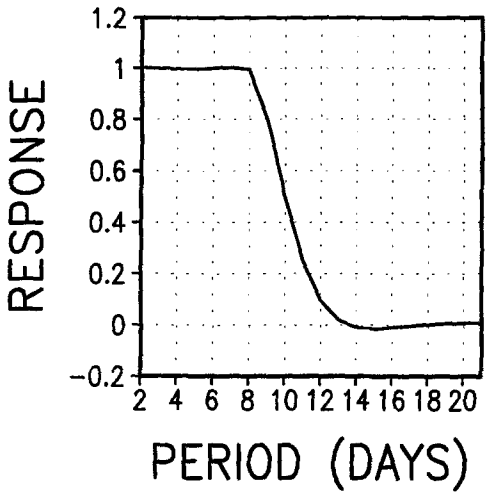

Fig. 1. Lanczos high-pass filter

on the data in the two midlatitude (30° S to 70° S) areas: the zonally global domain and the western hemisphere. The high-frequency anomalous 250-hPa meridional wind patterns are similarly determined using the data in the western hemisphere between 15° N and 70° S. All these areas are partially superimposed to investigate the connections of the high-frequency variability of the regional domain to that of the zonally global domain. In order to overcome computational limitations, the resolution of the original data is reduced by sampling the time series every other longitude, yielding a workable resolution of 5° in longitude by 2.5° in latitude, and using only the data for the 1990–1994 period.

The EOF calculations, based on the correlation matrix, are done separately for austral winter and summer. The physically meaningful identity of a given mode is assessed using the method proposed by North et al. (1982) accordingly to which two adjacent modes may be combined to yield a physically meaningful pattern if their eigenvalues are clustered, but well separated from their neighboring ones.

3. Results

3.1 The 500-hPa Geopotential Height Patterns in the Zonally Global Domain Between 30° S and 70° S

The first four austral winter modes explain respectively 6.9%, 6.7%, 6.3% and 6.1% and

the first four summer modes, 7.3%, 7.1%, 5.3% and 5.1% of the corresponding total high-frequency seasonal variances. Accordingly to the mode separation method (North et al., 1982), the winter modes are not well separated from each other. However, their patterns indicate that the pairs first/second and third/fourth modes describe two distinct modes of variability. The first/second and third/fourth summer modes have eigenvalues well separated from their corresponding neighboring ones. For these reasons and for brevity only the first and third modes of each analysis (austral winter and summer) are discussed.

3.1.1 Winter

The first winter eigenvector of the 500-hPa geopotential height (Fig. 2a) depicts a zonal wavenumber 4 wavetrain pattern around the SH midlatitudes with its largest loadings in the eastern hemisphere, generally centered to the south of 45° S. This feature is in agreement with previous studies on the path of transient systems over the SH. The storm tracks in the SH are mainly in the eastern hemisphere, where a maximum eddy kinetic energy has been observed (Hoskins et al., 1983; Trenberth, 1991). In the western hemisphere, a north-south dipole in the

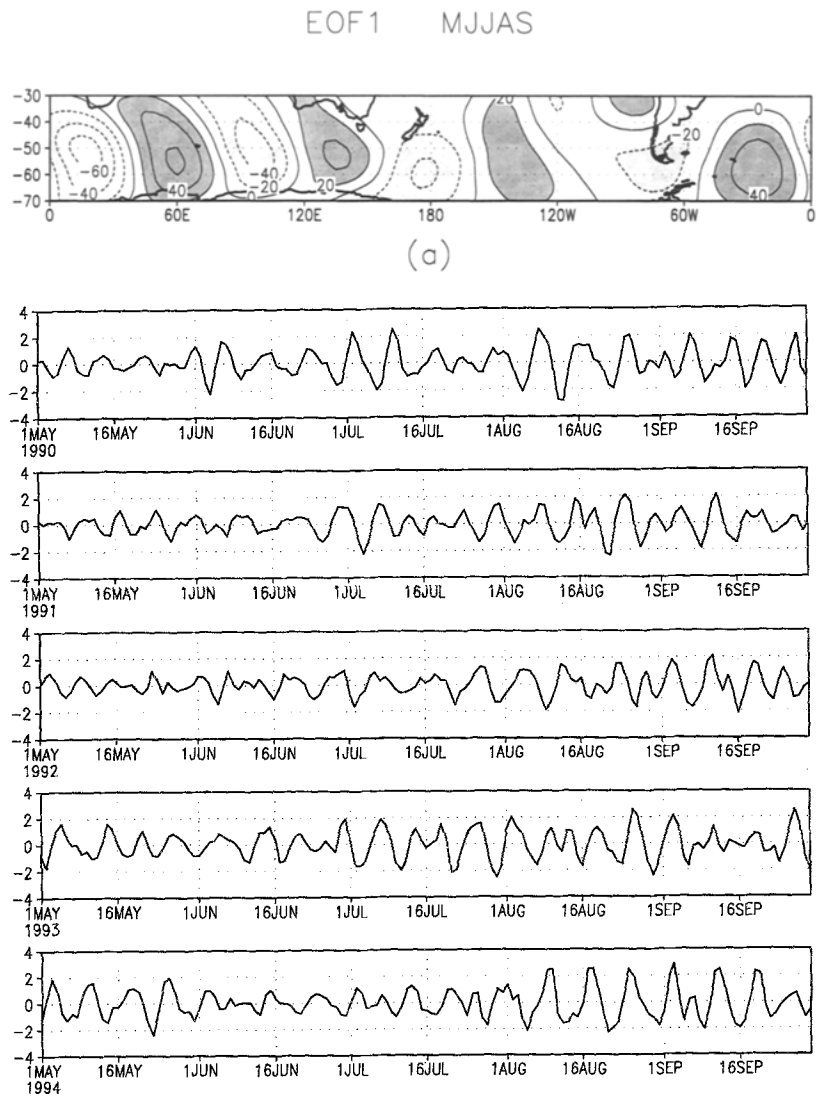

Fig. 2. The first austral winter mode patterns of the 500-hPa geopotential height in the zonally global domain in the SH midlatitudes (a) and the corresponding amplitude time series (b). The loadings have been multiplied by 100. The contour interval is 20. The loadings are contoured with positive (negative) values indicated by solid (dashed) lines. Darker (lighter) shading indicates values greater (less) than 20 (−20)

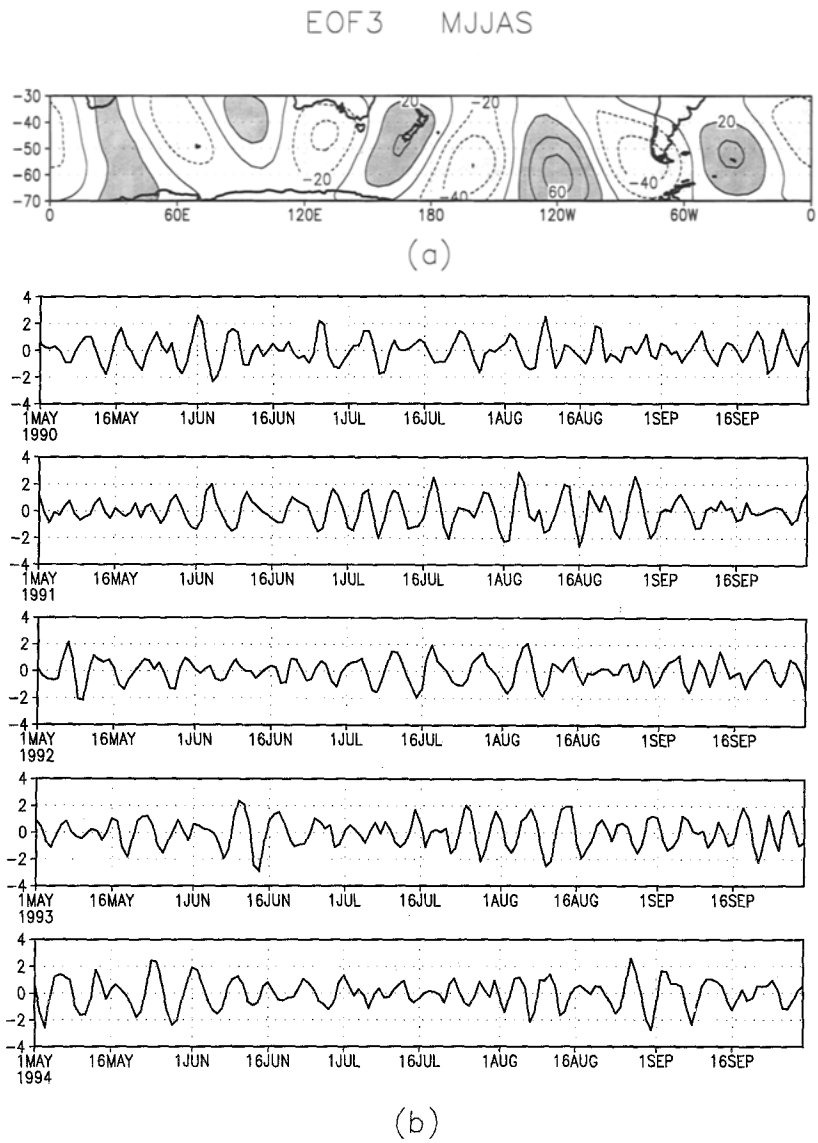

Fig. 3. The third austral winter mode patterns of the 500-hPa geopotential height in the zonally global domain in the SH midlatitudes (a) and the corresponding amplitude time series (b). Display is the same as that in Fig. 2

South American sector resembles a blocking configuration, which is a common feature of the winter circulation in this region (Kayano and Kousky, 1990). The corresponding amplitude time series (Fig. 2b) exhibits oscillations with periods from 5 to 8 days, which happens to be the time-scale of midlatitude synoptic systems, such as cyclones and anticyclones associated with cold fronts. Regarding the entire SH midlatitude these systems are relatively stronger in the eastern hemisphere than elsewhere, as shown by the first mode patterns of the 500-hPa geopotential height anomalies.

The third winter eigenvector (Fig. 3a) also shows a wavetrain in the SH midlatitudes featuring a zonal wavenumber 5 pattern with the largest loadings in the western hemisphere close to South America. The wavetrain path is concave (anticyclonic curvature) over the Pacific and convex over the Atlantic and Indian Oceans which resembles the arch pattern of Rossby waves, previously discussed by Hoskins (1983). The largest positive loadings centered at (60° S, 120° W) are flanked by negative loadings to the west and east. The eastern negative loadings extend over the southern tip of South America. The amplitude time series of this mode (Fig. 3b) shows high-frequency oscillations superimposed on synoptic-scale ones. Therefore, this mode describes the anomalous 500-hPa geopotential height patterns related to the synoptic systems, such as the cold fronts moving through the Pacific

Ocean, crossing the southern South America and reaching the Atlantic Ocean, as well as those related to the transient short waves. These systems are responsible for changes in the weather conditions over the southern South America (e.g., Kousky and Cavalcanti, 1997).

Additional analyses for the amplitude time series of these two modes (Figs. 2b and 3b) reveal interesting aspects of the temporal behavior of their corresponding patterns. The largest amplitudes of both modes occur more frequently at a nearly constant interval of 2 to 6 subsequent maxima (or minima) for certain periods. The subsequent maximum (or minimum) amplitudes of the first mode occur approximately at every 7 to 8 days during August 1990, July–August 1993 and August–September 1994. Concerning the third mode, its largest amplitudes are observed during the periods: 16 May–15 June, 1990; 16 July–30 August, 1991; July 1992; June and 16 July–16 August 1993; May and September 1994. In this case, the subsequent maximum (or minimum) amplitudes appear at an interval of 5 to 6 days, implying a higher frequency variability of the third mode. These results suggest that the intense SH midlatitude synoptic systems during winter are more likely to occur in sequences at a nearly constant interval of 5 to 8 days rather than intermittently.

3.1.2 Summer

The first summer eigenvector of the 500-hPa geopotential height (Fig. 4a) depicts a zonal

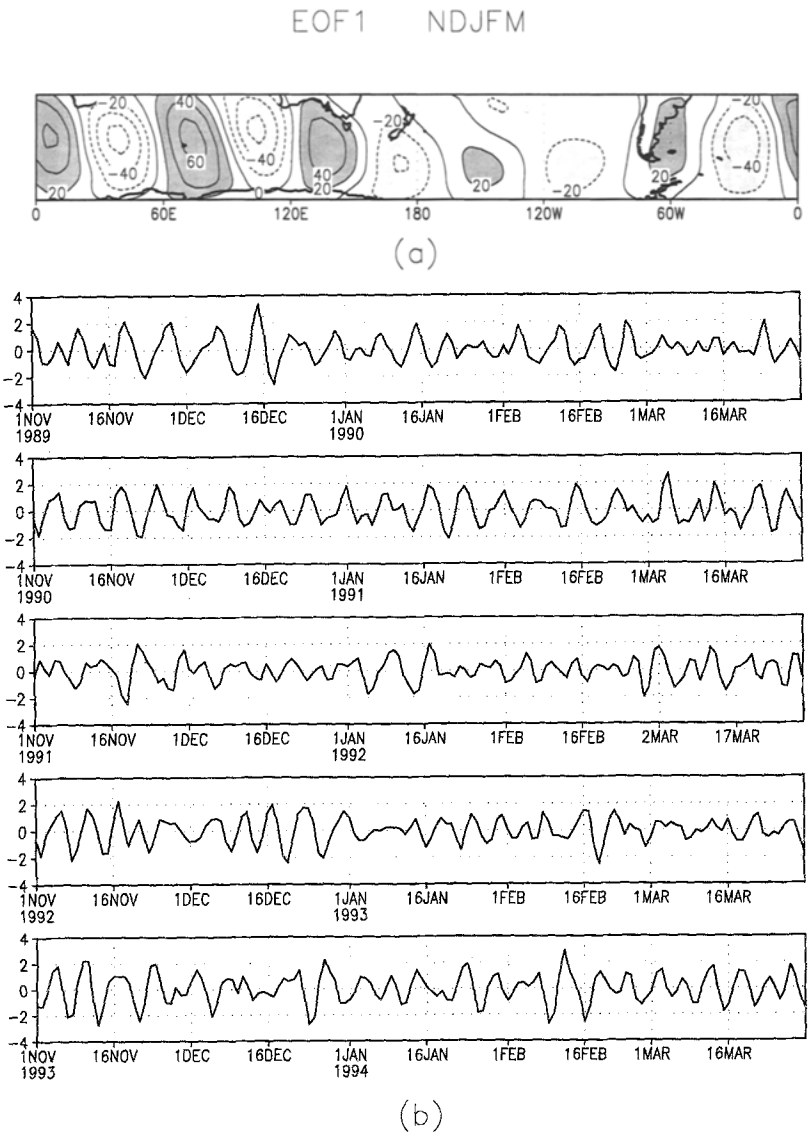

Fig. 4. The first austral summer mode patterns of the 500-hPa geopotential height in the zonally global domain in the SH midlatitudes (a) and the corresponding amplitude time series (b). Display is the same as that in Fig. 2

wavenumber 5 wavetrain structure in the SH midlatitudes with its largest loadings in the eastern hemisphere centered approximately at 45° S, in particular in areas west of 120° E, thus slightly shifted to the north of those for the first winter mode. The loadings in the western hemisphere are considerably smaller, except those over Atlantic which are in fact part of the eastern hemisphere pattern. The amplitude time series of the first summer mode (Fig. 4b) exhibits fluctuations with periods of 4 to 7 days. Thus this mode can be interpreted as anomalous 500-hPa geopotential height patterns in the eastern SH associated with the midlatitude synoptic systems.

The third summer eigenvector (Fig. 5a) shows a zonal wavenumber 6 wavetrain pattern with its largest loadings confined to the SH midlatitudes extending from 120° E eastward to the Greenwich meridian, with a concave path in this region. The South American sector wavetrain pattern has a northeastward extension with the positive loadings over the southern and negative ones over Southwestern Atlantic, what might indicate the presence of SACZ, a summer feature shown by Kodama (1992) to be related to frontal systems. The amplitude time series of this mode (Fig. 5b) exhibits synoptic-scale as well as higher frequency oscillations. The pattern displayed in Fig. 5a thus reflect the anomalous atmospheric summer circulation in the western SH related to midlatitude synoptic systems and transient short waves.

Likewise the winter modes, the largest values of the amplitude time series of the summer

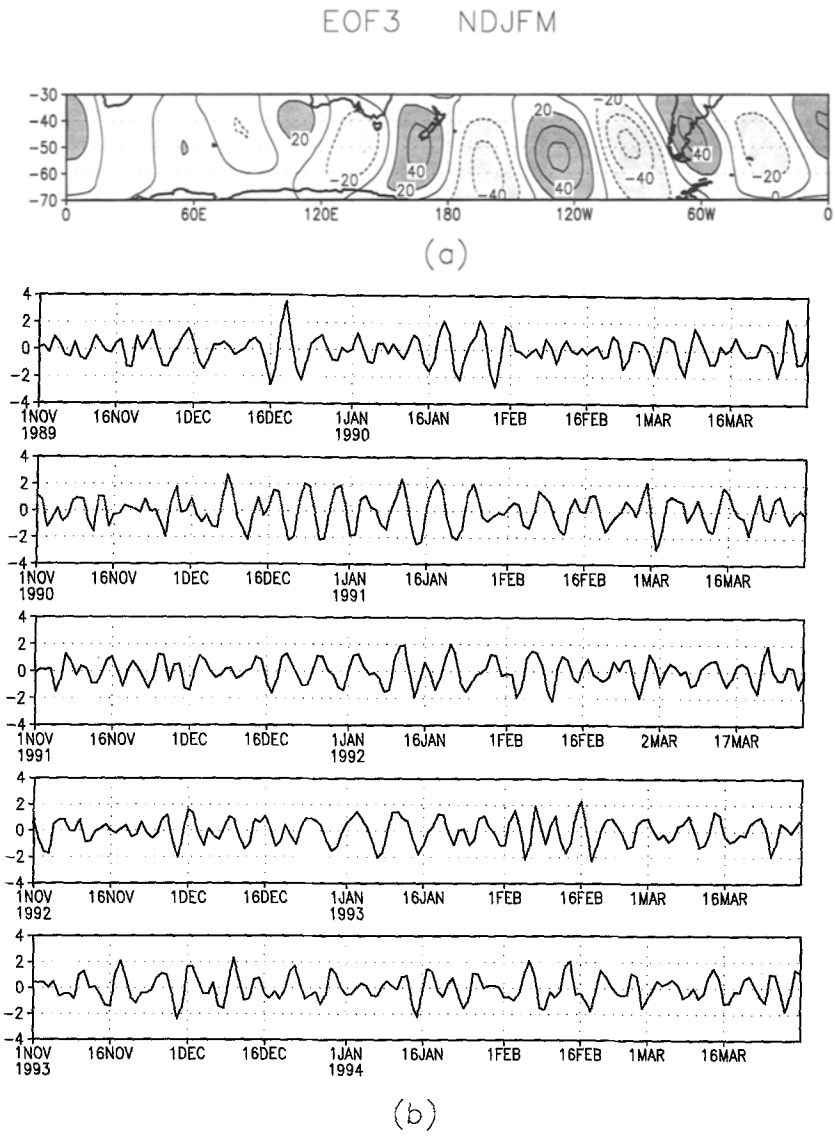

Fig. 5. The third austral summer mode patterns of the 500-hPa geopotential height in the zonally global domain in the SH midlatitudes (a) and the corresponding amplitude time series (b). Display is the same as that in Fig. 2

modes (Figs. 4b and 5b) occur in general at a nearly constant interval of 2 to 6 subsequent maxima (or minima) for some periods. Thus, the intense summer midlatitude synoptic systems also appear preferably in a sequential manner.

3.2 The 500-hPa Geopotential Height Patterns in the Western Hemisphere Between 30° S and 70° S

The EOF analyses of 500-hPa geopotential height in the western SH midlatitudes are discussed in this section. The percentage of the total high-frequency seasonal variances explained by the first four austral winter modes are: 10.9%, 10.5%, 8.3% and 7.9% and by the first four summer modes, 9.6%, 9.2%, 6.6% and 6.1%, respectively. For both seasons, the first/second and the third/fourth modes form two pairs whose eigenvalues are well separated from their corresponding neighboring ones. As before, only the first and third modes of each analysis are discussed.

3.2.1 Winter

The first winter eigenvector of the 500-hPa geopotential height (Fig. 6a) features a well organized wavetrain pattern in the SH midlatitudes with its centers lying on a concave path from central and eastern Pacific toward the Atlantic Ocean. This pattern contains the same regional features of the third winter mode for the case of the zonally global domain (Fig. 3a). The

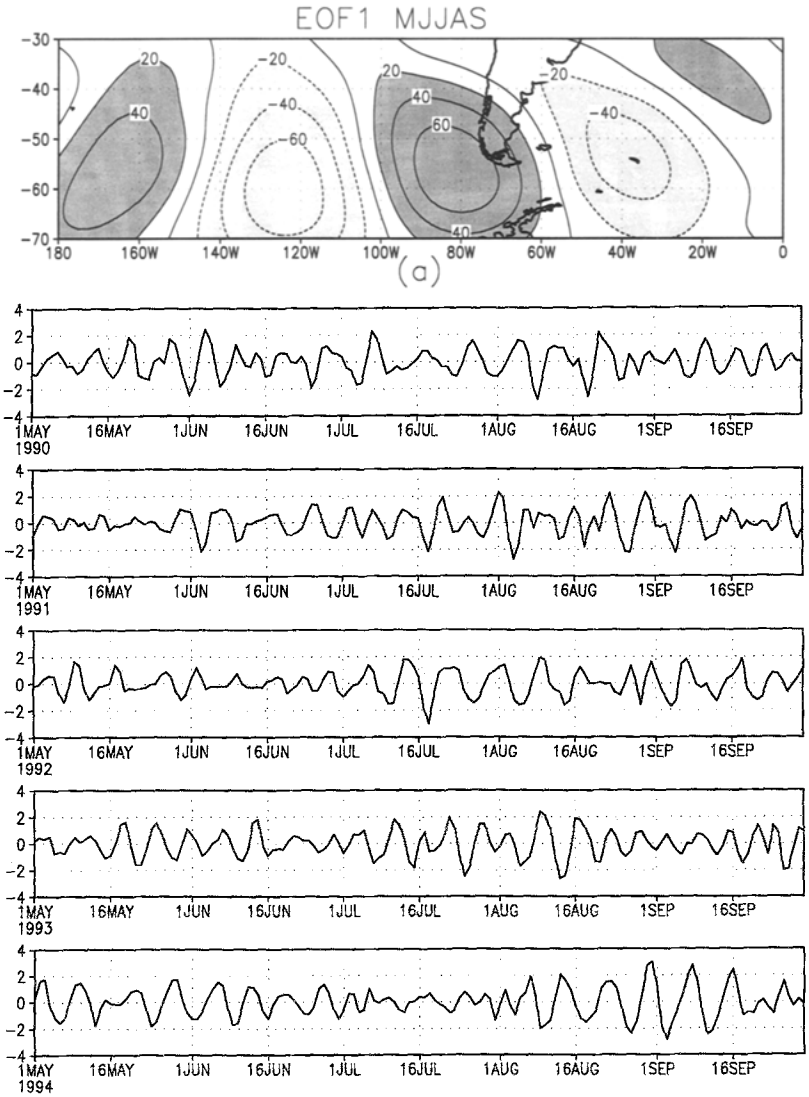

Fig. 6. The first austral winter mode patterns of the 500-hPa geopotential height in the western SH midlatitudes (a) and the corresponding amplitude time series (b). Display is the same as that in Fig. 2

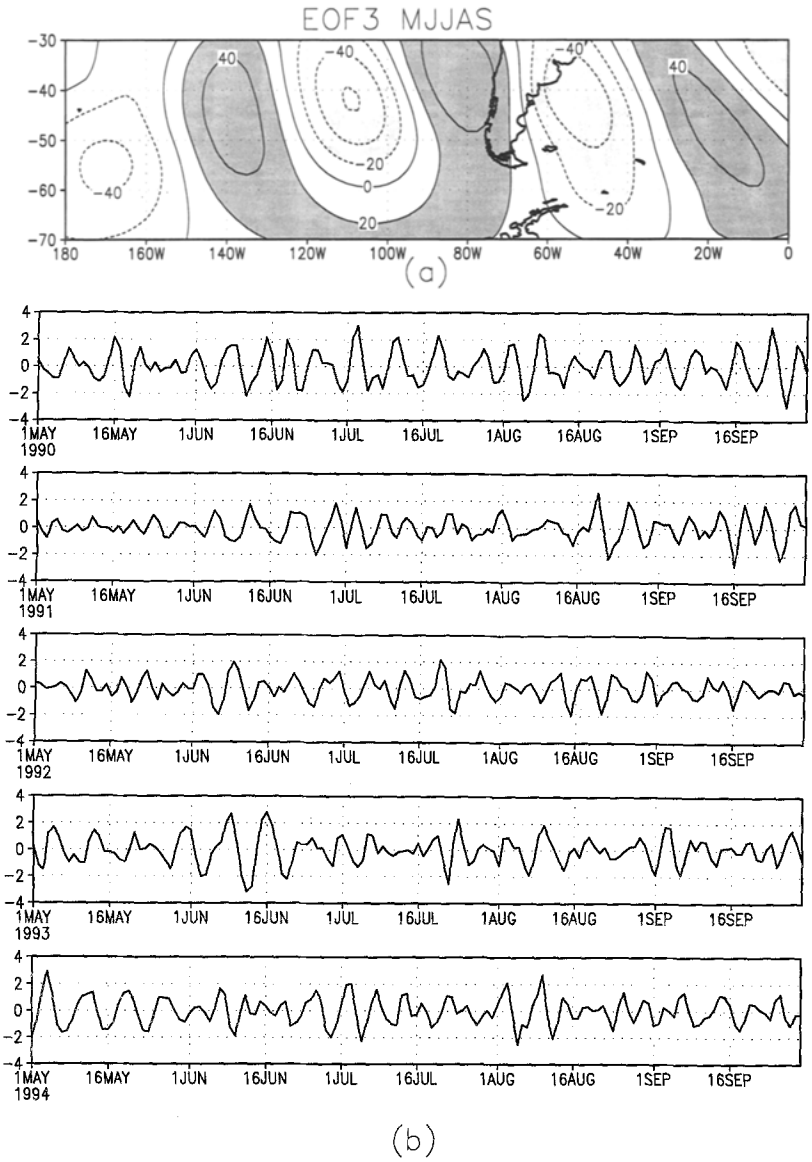

Fig. 7. The third austral winter mode patterns of the 500-hPa geopotential height in the western SH midlatitudes (a) and the corresponding amplitude time series (b). Display is the same as that in Fig. 2

amplitude time series of first winter mode (Fig. 6b) have high-frequency superimposed on synoptic-scale fluctuations. This mode represents the troughs and ridges of either frontal systems or transient short waves which change the weather conditions in the southern and southeastern South America. The nearly zonal dipole pattern (a ridge and a trough) over these regions is a feature associated with a longwave normally present in frost events or when cold outbreaks occur in the Amazon.

The third winter eigenvector (Fig. 7a) also depicts a wavetrain structure with its centers along a convex (cyclonic) path from central South Pacific to the South Atlantic Ocean followed by a northeastward extension. In the South American sector the largest loadings extend mostly over areas south to 30° S. The synoptic and higher frequency fluctuations in the amplitude time series of this mode (Fig. 7b) indicates that it represents the 500-hPa geopotential height anomalies related to the passage of troughs and ridges of the frontal zones and transient short waves that cross the southern South America.

3.2.2 Summer

The first summer eigenvector of the 500-hPa geopotential height (Fig. 8a) features a wavetrain oriented in the southwest-northeast direction, with its largest loadings over the southern South

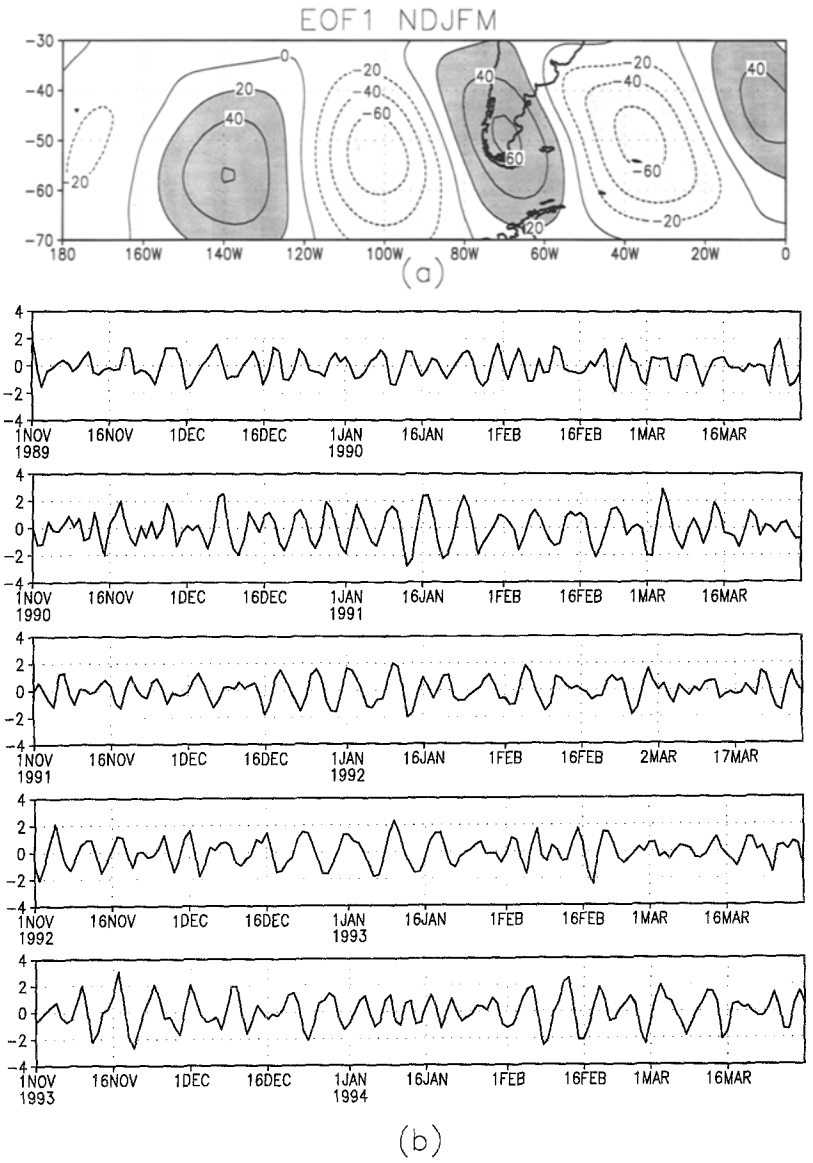

Fig. 8. The first austral summer mode patterns of the 500-hPa geopotential height in the western SH midlatitudes (a) and the corresponding amplitude time series (b). Display is the same as that in Fig. 2

America and neighboring oceanic areas. This wavetrain is the regional pattern of the third summer mode shown in Fig. 5a. The largest amplitude of the first summer mode (Fig. 8b) occur mainly at the synoptic scale, although higher frequency oscillations are also noted for some periods. Therefore this mode describes the anomalous 500-hPa geopotential height patterns related mostly to the synoptic systems.

The third summer eigenvector (Fig. 9a) shows a wavetrain pattern with its centers lying on a convex path in the area between 140° W and 20° W. Its loadings are relatively smaller than those of the first mode of this analysis, meaning that the waves are weaker than those for the first mode. The amplitude time series of the third summer mode shows high-frequency fluctuations superimposed on those of the synoptic-scale (Fig. 9b).

As in the previous 500-hPa geopotential height analyses for the zonally global domain in the SH midlatitudes, the amplitude times series for the regional summer and winter modes show sequences of 2 to 5 maxima (or minima) at a nearly constant interval for certain periods. It is worthy noting that the amplitude time series of the third summer mode shows only a few (2 to 3) subsequent maximum (or minimum) values, what suggests a higher frequency variability of this mode. Thus, the intense synoptic systems in the western SH are more common to occur sequentially than intermittently.

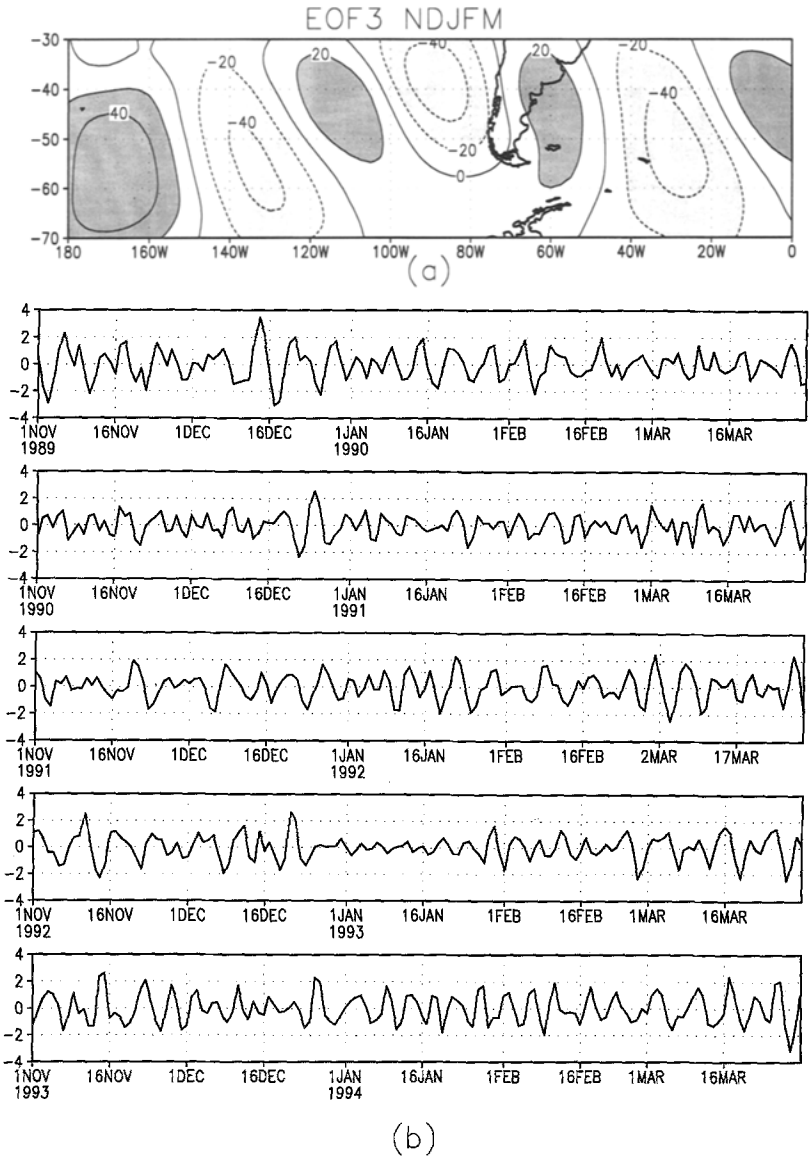

Fig. 9. The third austral summer mode patterns of the 500-hPa geopotential height in the western SH midlatitudes (a) and the corresponding amplitude time series (b). Display is the same as that in Fig. 2

3.3 The 250-hPa Meridional Wind Patterns in the Western Hemisphere Between 15° N and 70° S

This work focuses on the SH midlatitude high-frequency systems and their connections to the weather of the extratropical and tropical South America. The 250-hPa meridional wind is the variable chosen for the EOF analyses in the western hemisphere between 15° N and 70° S. Such a choice is justified because the inclusion of tropical and extratropical geopotential height data in an EOF analysis could yield non-physical patterns since the geopotential perturbations associated with equatorial synoptic-scale disturbances are an order of magnitude smaller than those for midlatitude synoptic systems.

The percentage of the total high-frequency seasonal variances explained by the first four austral winter modes are: 6.1%, 6.0%, 5.8% and 5.4% and by the first four summer modes, 5.8%, 5.5%, 4.3% and 4.1%, respectively. Additional analyses of the first four EOF patterns for each season indicate that the first/second and the third/fourth modes form pairs whose eigenvalues are separated from their neighboring ones. Thus, for both seasons only the first and third modes are discussed in this section, as before.

3.3.1 Winter

The first winter eigenvector of the 250-hPa meridional wind (Fig. 10a) shows the largest loadings in the southeastern Pacific which

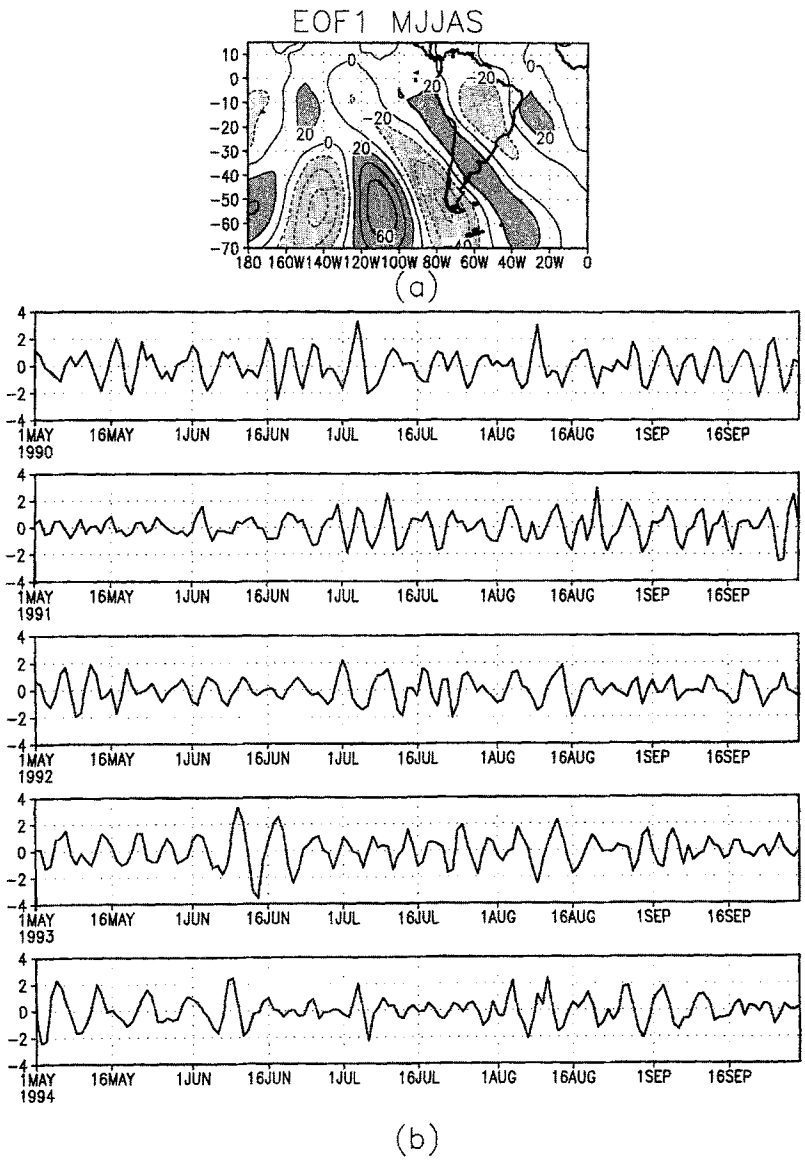

Fig. 10. The first austral winter mode patterns of the 250-hPa meridional wind in the western hemisphere between 15° N and 70° S (a) and the corresponding amplitude time series (b). Display is the same as that in Fig. 2

resemble the regional 500-hPa geopotential height wavetrain pattern in the SH midlatitudes (see Figs. 3a and 6a). This pattern describes the passage of troughs and ridges associated with frontal systems. The meridional wind pattern shows a northeastward extension over South America. The amplitude time series of this mode (Fig. 10b) contains synoptic and short time-scale fluctuations. This mode describes the winter 250-hPa meridional wind anomalies related to cold fronts and transient short waves that move through South America, affecting the weather in the interior of the continent. In these cases, frosts might occur in the southern and southeastern parts of the continent and occasionally cold outbreaks might be observed in the Amazon. The positive loadings extending northwestward from southern and southeastern South America toward the southern Amazon are indicative of the influence of SH midlatitude high-frequency systems on tropical areas, as in the case of cold outbreaks in the Amazon.

The third winter mode eigenvector (Fig. 11a) shows its largest loadings south to 15° S in a wavetrain pattern extending zonally from the subtropical eastern Pacific to southern South America and from there northeastward into the Atlantic. The amplitude time series of this mode (Fig. 11b) shows synoptic and short time-scale fluctuations. This mode describes the upper level meridional wind anomalies caused by transient and synoptic waves that cross the southern

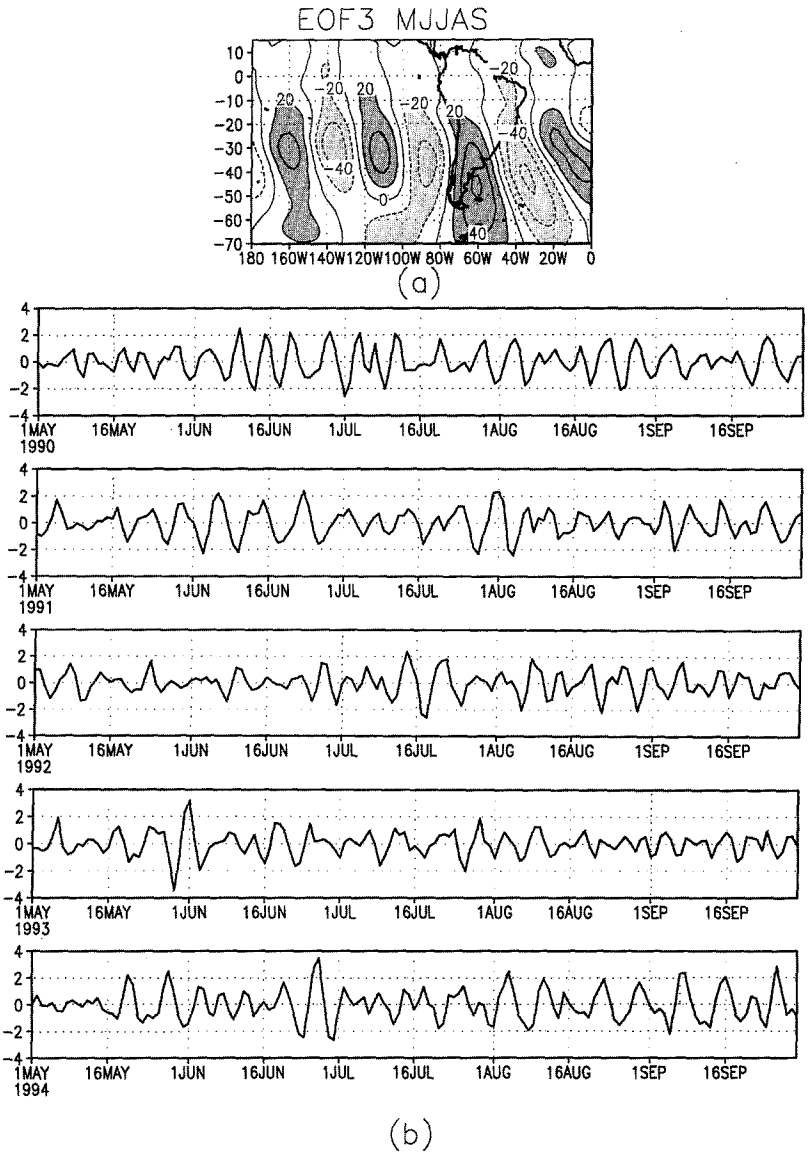

Fig. 11. The third austral winter mode patterns of the 250-hPa meridional wind in the western hemisphere between 15° N and 70° S (a) and the corresponding amplitude time series (b). Display is the same as that in Fig. 2

South America. Quite often these systems cause cyclogeneses over southeastern South America (Gan and Rao, 1994). This mode may also represent the upper level cyclonic vortices moving from subtropical eastern Pacific toward South America.

3.3.2 Summer

The first summer eigenvector of the 250-hPa meridional wind (Fig. 12a) features a nearly zonally oriented wavetrain pattern mostly confined to the SH midlatitudes. The northeastward extension of the loadings is evident in the South American region, what is indicative of wave pulses from the frontal systems responsible for the maintenance of convective activity in the SACZ. The amplitude time series of this mode (Fig. 12b) also shows synoptic and short time-scale fluctuations.

The third summer mode (Fig. 13a) exhibits a wavetrain pattern along a nearly convex path from South Pacific to South Atlantic over the southern South America. This mode probably represents the 250-hPa meridional wind anomalies caused by the upper level cyclonic vortices originating in the subtropical Pacific, which are frequently observed during the austral summer (Kousky and Gan, 1981). The amplitude time series of this mode (Fig. 13b) is relatively noisier than the corresponding one of the first mode in this analysis. This suggests that the systems

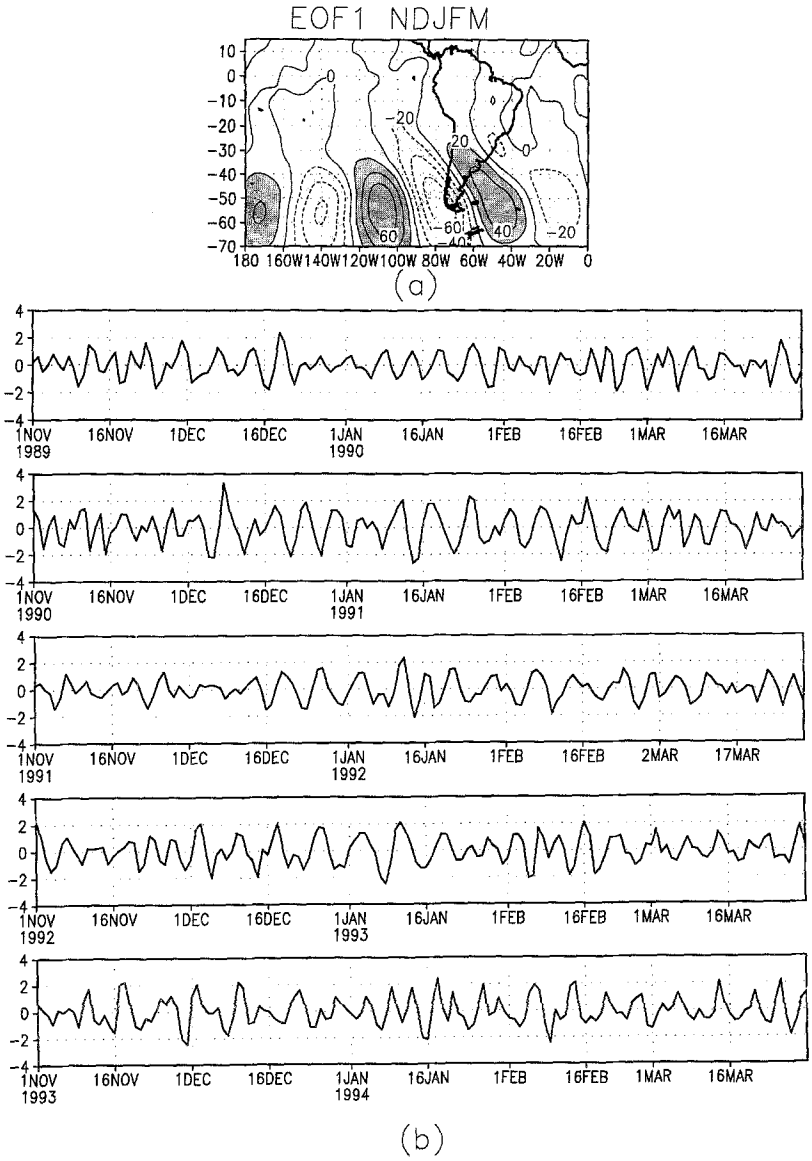

Fig. 12. The first austral summer mode patterns of the 250-hPa meridional wind in the western hemisphere between 15° N and 70° S (a) and the corresponding amplitude time series (b). Display is the same as that in Fig. 2

associated with the third summer mode are predominantly the high-frequency systems.

4. Concluding Remarks

Daily 500-hPa geopotential height and 250-hPa meridional wind reanalyzed data obtained from the National Centers for Environmental Prediction were used to document the austral winter and summer high-frequency variability in the SH midlatitudes and in particular, over the South American sector for the 1990–1994 period. The high-frequency patterns were determined by performing separated EOF analyses for each of these variables in selected areas. The geopotential data were for the zonally global domain and the western hemisphere within it, bounded by the 30° S and 70° S. The meridional wind data were for the region between 15° N and 70° S in the western hemisphere. Analyses for winter and summer were done separately, with the patterns corresponding to the first and third mode of each analysis being discussed in detail.

The dominant 500-hPa geopotential height patterns in the zonally global domain (Figs. 2a and 4a) feature, for both seasons, a wavetrain structure with zonal wavenumber 4 for winter, and 5 for summer with the wave amplitudes being larger in the eastern hemisphere. In agreement, Hoskins et al. (1983) and Trenberth (1991) identified the eastern SH as the region of the storm tracks, where they found a maximum

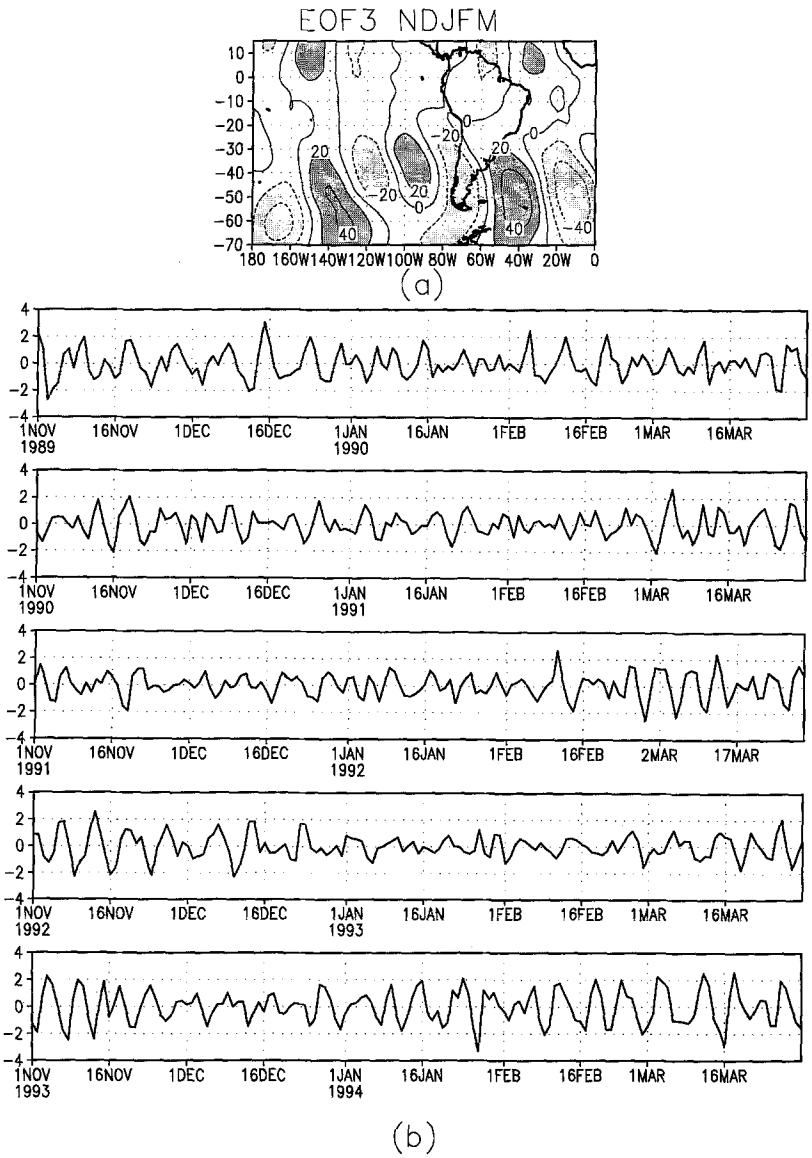

Fig. 13. The third austral summer mode patterns of the 250-hPa meridional wind in the western hemisphere between 15° N and 70° S (a) and the corresponding amplitude time series (b). Display is the same as that in Fig. 2

eddy kinetic energy. The secondary patterns (third modes) for this variable feature a wavetrain structure with zonal wavenumber 5 for winter and 6 for summer with centers more intense in the southeastern Pacific and southern South America for both seasons. The amplitude times series of the first winter and summer modes show a dominance of the synoptic-scale fluctuations and those of the third modes contain additional short time-scale fluctuations. Thus the first winter and summer modes represent synoptic systems, such as cyclones and anticyclones associated with midlatitude cold fronts. The third modes are associated with synoptic-scale systems and transient short waves.

The anomalous 500-hPa geopotential height patterns in the western SH midlatitudes, given by the first winter and summer modes, contain the regional features of the third winter and summer modes of the analyses for the zonally global domain. The amplitude time series of these modes exhibit high-frequency superimposed on synoptic fluctuations. The regional modes represent the troughs and ridges associated either with frontal systems or transient short waves all of which cause changes in the weather of the southern and southeastern South America. Indeed, the first winter pattern resembles that associated with a longwave frequently observed when frosts occur in these regions or when a cold front reaches the Amazon region. The two modes presented for each season describe two distinct modes of high-frequency variability. The wavetrain of the first mode for each season has a

northeastward extension over southern South America. The part of the wavetrain of the two third modes over South America for each season shows a nearly zonal pair of opposite sign centers located slightly to the north of those for the corresponding first modes. Therefore, the first and third modes of each analysis describe different aspects of the high-frequency variability.

The first winter and summer patterns of the 250-hPa meridional wind show a wavetrain over southeastern Pacific, as noted in the 500-hPa geopotential height analyses. However, this wavetrain extends equatorward over the South American continent, in particular during winter. This feature might be indicative of the cold outbreaks in the southern Amazon during winter, and of the variations in the SACZ caused by wave pulses in the frontal systems during summer.

It is worthwhile pointing out that the analyses for the 1985–1989 data (not shown) reproduced the same results as those discussed in this paper. This gives more confidence on the results presented here which do not depend on the particular period chosen. Finally, an important point considered in this paper concerns the behavior of intense synoptic systems in the eastern and southeastern Pacific, which clearly occur in sequences for certain periods at a nearly constant interval instead of appearing intermittently. This result might be of use for daily weather forecasts, in particular for the southern South America. However to confirm its applicability for practical purposes operational tests must still be conducted.

Acknowledgements

The authors were partially supported by the Conselho Nacional de Desenvolvimento Científico and Tecnológico of Brazil.

References

Berbery, E. H., Vera, C. S., 1996: Characteristics of the Southern hemisphere winter storm track with filtered and unfiltered data. *J. Atmos. Sci.*, **53**, 468–481.

Duchon, C. E., 1979: Lanczos filtering in one and two dimensions. *J. Appl. Meteor.*, **18**, 1016–1022.

Gan, M. A., Rao, V. B., 1991: Cyclogenesis over South America. *Mon. Wea. Rev.*, **119**, 1293–1302.

Gan, M. A., Rao, V. B., 1994: The influence of the Andes Cordillera on transient disturbances. *Mon. Wea. Rev.*, **122**, 1141–1157.

Hoskins, B. J., 1983: Dynamical processes in the atmosphere and the use of models. *Quart. J. Roy. Meteor. Soc.*, **109**, 1–21.

Hoskins, B. J., James, I. N., White, G. H., 1983: The shape, propagation and mean flow interaction of large-scale weather systems. *J. Atmos. Sci.*, **40**, 1595–1612.

Kalnay, E., et al., 1996: The NCEP/NCAR 40-year reanalysis project. *Bull. Amer. Meteor. Soc.*, **77**, 437–471.

Kayano, M. T., Kousky, V. E., 1990: Southern hemisphere blocking: a comparison between two indices. *Meteorol. Atmos. Phys.*, **42**, 165–170.

Kayano, M. T., Ferreira, N. J., Ramirez, M. C. V., 1997: Summer circulation patterns related to the upper tropospheric vortices over the tropical South Atlantic. *Meteorol. Atmos. Phys.*, **64**, 203–213.

Kodama, Y., 1992: Large-scale common features of subtropical precipitation zones (the Baiu frontal zone, SPCZ, and the SACZ)–Part I: Characteristics of subtropical frontal zones. *J. Meteor. Soc. Japan*, **70**, 813–836.

Kousky, V. E., 1979: Frontal influences on northeast Brazil. *Mon. Wea. Rev.*, **107**, 1140–1153.

Kousky, V. E., Cavalcanti, I. F. A., 1997: The principal modes of high-frequency variability over the South American region. Preprints of the Fifth International Conference on Southern Hemisphere Meteorology and Oceanography, Pretoria, South Africa, 7–11 April, 226–227.

Kousky, V. E., Gan, M. A., 1981: Upper tropospheric cyclonic vortices in the tropical South Atlantic. *Tellus*, **33**, 538–551.

North, G. R., Bell, T. L., Cahalan, R. F., Moeng, F. J., 1982: Sampling errors in the estimation of empirical orthogonal functions. *Mon. Wea. Rev.*, **110**, 699–706.

Sinclair, M. R., 1996: A climatology of anticyclones and blocking for the Southern hemisphere. *Mon. Wea. Rev.*, **124**, 245–263.

Trenberth, K. E., 1981: Observed Southern Hemisphere eddy statistics at 500-mb frequency and spatial dependence. *J. Atmos. Sci.*, **38**, 2585–2605.

Trenberth, K. E., 1982: Seasonality in Southern hemisphere eddy statistics at 500-mb. *J. Atmos. Sci.*, **39**, 2507–2520.

Trenberth, K. E., 1991: Storm track in the Southern hemisphere. *J. Atmos. Sci.*, **48**, 2159–2178.

Virji, H., 1981: A preliminary study of summertime tropospheric circulation patterns over South America estimated from cloud winds. *Mon. Wea. Rev.*, **109**, 599–610.

Authors' addresses: Iracema F. A. Cavalcanti, Instituto Nacional de Pesquisas Espaciais, CPTEC, Rodovia Presidente Dutra, Km 40 SP/RJ 12630-000 Cachoeira Paulista, SP, Brazil, (e-mail: iracema@cptec.inpe.br); Mary T. Kayano, Instituto Nacional de Pesquisas Espaciais, DCM, Avenida dos Astronautas 1758, 12227-010 São José dos Campos, SP, Brazil, (e-mail: mary@met.inpe.br).